Title: Hematopoietic stem cells differentiate into restricted myeloid progenitors before cell division

Authors: Tatyana Grinenko[1*], Anne Eugster[2], Lars Thielecke[3], Beata Ramazs[1], Anja Krueger[1], Sevina Dietz[2], Ingmar Glauche[3], Alexander Gerbaulet[4], Malte von Bonin[5,6,7], Onur Basak[8,9], Hans Clevers[8,9,10], Triantafyllos Chavakis[1,2], Ben Wielockx[1,2*]

Affiliations:

[1]Department of Clinical Pathobiochemistry, Institute for Clinical Chemistry and Laboratory Medicine, Technische Universität, Dresden, Germany.

[2]DFG Research Centre and Cluster of Excellence for Regenerative Therapies Dresden, Technische Universität Dresden, Germany,

[3]Institute for Medical Informatics and Biometry (IMB), Technische Universität Dresden, Germany.

[4]Institute for Immunology, Technische Universität, Dresden, Germany.

[5]Medical Clinic and Policlinic I, University Hospital Carl Gustav Carus, Technische Universität Dresden, Dresden, Germany.

[6]German Cancer Consortium (DKTK), partner site Dresden, Germany.

[7]German cancer research center (DKFZ), Heidelberg, Germany.

[8]Hubrecht Institute, Royal Netherlands Academy of Arts and Sciences and University Medical Center Utrecht, 3584 CT, Utrecht, the Netherlands.

[9]Cancer Genomics Netherlands, UMC Utrecht, 3584 GC, Utrecht, the Netherlands.

[10]Princess Máxima Centre, 3584 CT Utrecht, the Netherlands.

***Correspondence to:** tatyana.grinenko@uniklinikum-dresden.de, ben.wielockx@tu-dresden.de

Summary

Hematopoietic stem cells (HSCs) continuously replenish all blood cell types through a series of differentiation steps that involve the generation of lineage-committed progenitors as well as necessary expansion due to repeated cell divisions. However, whether cell division in HSCs precedes differentiation is unclear. To this end, we used an HSC cell tracing approach and $Ki67^{RFP}$ knock-in mice to assess simultaneously divisional history, cell cycle progression, and differentiation of adult HSCs *in vivo*. Our results reveal that HSCs are able to differentiate into restricted progenitors, especially common myeloid progenitors, restricted megakaryocyte-erythroid progenitors (PreMEs) and pre-megakaryocyte progenitors (PreMegs), without undergoing cell division and even before entering the S phase of the cell cycle. Additionally, the phenotype of the undivided but differentiated progenitors correlated with expression of lineage-specific genes that manifested as functional differences between HSCs and restricted progenitors. Thus, HSC fate decisions appear to be uncoupled from physical cell division. These results facilitate a better understanding of the mechanisms that control fate decisions in hematopoietic cells. Our data, together with separate findings from embryonic stem cells, suggest that cell division and fate choice are independent processes in pluripotent and multipotent stem cells.

Introduction

A rare population of hematopoietic stem cells (HSCs) resides at the top of the hematopoietic hierarchy [1]. Although most adult HSCs normally exist in a quiescent or dormant state [2], some of them divide and support the production of all mature blood cell types through multiple intermediate progenitor stages, during steady state and in response to acute needs [3-5]. This classical point of view was questioned in recent studies from two groups showing that HSC populations contain stem-cell like megakaryocyte progenitors, which under stress conditions such as transplantation into irradiated recipients[6] or after acute inflammation[7], activate a megakaryocyte differentiation program. The commitment process(es) that turns

HSCs into mature cells are currently understood to be a sequence (or even a continuum) of decision steps in which the multi-lineage potential of the cells is sequentially lost [8-10]. Although many of these steps have been investigated in great detail, the entire picture is still repeatedly challenged [6,8,9,11-13]. HSC transition through the multipotent and restricted progenitor stages is also accompanied by intense cell proliferation [3]. However, it is unclear whether each fate decision step is associated with one or more division events, or if cell proliferation and differentiation are independent processes. Further, if differentiation of HSCs does require cell division, the phase of the cell cycle that is particularly important for this process is also currently unknown. The dependence of cell-fate decisions on cell cycle progression was so far only shown *in vitro* for pluripotent embryonic stem cells [14-17]. However, a few reports point toward a functional connection between these two processes in adult stem cells, such as neuronal stem cells [16,18]. With regard to hematopoietic stem and progenitor cells, characterization of the cell cycle itself is currently ongoing [19-22], and an understanding of how HSC fate decisions relate to cell division and cell cycle progression is lacking [19].

Therefore, we used *in vivo* cell tracing to simultaneously follow the divisional history and the initial differentiation steps of HSCs. Our data reveal that HSCs are able to differentiate into restricted progenitors prior to cell division, most prominently megakaryocyte-erythroid progenitors (PreME) and pre-megakaryocyte progenitors (PreMeg), and that this occurs before the cells enter the S phase of the cell cycle. Moreover, our data also demonstrate that the G0/G1 phases are crucial for fate decision in HSCs to either differentiate or self-renew.

Results

HSCs differentiate into myeloid progenitors *in vivo* without undergoing cell division

To study the initial steps of HSC differentiation *in vivo*, we sorted Lin^- Kit^+ $Sca\text{-}1^+$ (LSK) $CD48^-$ $CD41^-$ $CD150^+$ stem cells (Figure 1a)[1]. $CD41^+$ cells were excluded to avoid myeloid- [23] and megakaryocyte-

biased HSCs [24-26]. We used the CellTrace Violet dye [27,28] to uniformly label HSCs and track cell-division history after transplantation (Figure 1a). Recently, Shimoto et al have shown that numerous empty HSC niches are available upon transplantation into non-conditioned recipients, which are located distant from filled niches and available for HSC engraftment and proliferation. Moreover, donor HSCs give rise to all blood cells without any bias[29]. Labelled cells were transplanted into unconditioned recipients to prevent irradiation-induced stress[30-32] (Figure 1a). Thirty-six hours after transplantation, 30% of the donor cells had downregulated Sca-1 expression (Figure 1b), one of the principal surface markers for HSCs[33], and changed their phenotype from HSCs to myeloid progenitors (MP). Importantly, the purification procedure alone did not lead to down-regulation of Sca-1 (Supplementary Figure 1a). A possible contamination of potential donor MPs was excluded, since transplantation of these progenitors alone did not result in any detectable donor MPs 36 hours later (Supplementary Figure 1b). To further classify these phenotypically restricted MPs *in vivo*, we used a previously described method of surface staining [34]; we initially confirmed its applicability after transplantation into lethally irradiated mice (Supplementary Figure 2a-b). Based on surface staining at 36 h post transplantation, we subdivided donor MPs into the following restricted progenitors: common myeloid progenitors (CMPs), granulocyte-macrophage progenitors (GMPs), pre-megakaryocyte-erythroid progenitors (PreMEs), and pre-megakaryocyte progenitors (PreMegs) (Figure 1b).

Next, we analyzed the proliferation history of transplanted cells based on dilution of CellTrace Violet dye, whereby intensity of the dye in $CD4^+CD62L^+$ naïve T cells was used as the reference for undivided cells (Supplementary Figure 1c) [35,36]. This analysis reveals that, at 36 hours after HSC transplantation, a majority of LSK cells with the long-term HSC phenotype (LSK $CD48^-$ $CD150^+$), short-term HSCs (ST-HSC) (LSK $CD48^-$ $CD150^-$), multipotent progenitors (MPP2: LSK $CD48^+$ $CD150^+$ and MPP3/4 LSK $CD48^+$ $CD150^-$) (Supplementary Figure 3a) [1] and 50% of the MPs remained undivided (Figure 1c). Additionally, based on CD41 and CD150 expression, these MPs were predominantly CMPs, PreMEs, and PreMegs (Figure 1d-e). We also performed an even more stringent gating strategy to avoid overlay

between non-divided and divided cells (Supplementary Figure 1d), but found no difference in the frequency of restricted progenitors, as compared to the previous gating strategy (Supplementary Figure 1e). To exclude the possibility that HSCs differentiated into MPs without division due to the limited niche space, we used the HSC-CreERT+R26$^{DTA/DTA}$ mouse line allowing for the inducible depletion of HSCs and transplanted CellTrace dye labelled wild type HSCs into them[37] (Supplementary Figure 1f). However, we did not find any difference in the frequency of HSCs differentiated into myeloid restricted progenitors 36h after transplantation, compared to controls (Supplementary Figure 1g-h). Surprisingly, compared to mice not preconditioned with tamoxifen (TAM), we found that donor HSCs in TAM treated mice displayed enhanced differentiation into GMPs without cell division, suggesting potentially additional stress induced by TAM.

Interestingly, transplantation of MPP2 or MPP3/4 subsets revealed a similar phenomenon as most of the MPs did not divide. Further, while MPP2 cells mostly gave rise to PreMEs and PreMeg cells, MPP3/4 cells differentiated into CMPs and GMPs (Supplementary Figure 3b-d). Taken together, these results strongly suggest that HSCs/MPPs can give rise to restricted progenitors including CMPs, PreMEs, and PreMegs based on the cell phenotype, without undergoing cell division.

Phenotype of undivided differentiated progenitors correlates with expression of lineage-specific genes

To investigate the molecular differences between undivided HSCs and undivided MPs, we designed a panel of primers to analyse single-cell expression levels of 70 genes including cell cycle genes and those specific for HSCs, myeloid, erythroid, megakaryocyte-erythroid progenitors (MEP) and platelets (Supplementary Table 1) [8,9,11,12,33,38-41]. Essentially, single-cell expression analysis of freshly sorted HSCs, CMPs, PreMEs and PreMegs showed a clear separation of the cell types whether based on all analyzed genes or only on selected MEP/Platelet genes (Supplementary Figure 4a-c).

We then isolated undivided donor cells at 36h after transplantation of LSK CD48$^-$ CD41$^-$ CD150$^+$ cells (Figure 2a) and retrospectively categorized them on the basis of index-sorting data as HSCs (LSK CD48$^-$ CD150$^+$) or various MP populations (Supplementary Figure 5a-d). Within these populations, we performed single-cell qPCR on 42 HSCs, 7 CMPs, 15 PreMEs, and 20 PreMegs, pooled and obtained from two independent experiments (Figure 2b). Performing t-distributed stochastic neighbor embedding (t-SNE) analysis of the qPCR data revealed separation of HSCs from PreMEs and PreMegs, based on all analysed genes (Figure 2c) or the MEP/Platelet genes alone (Figure 2d, Supplementary Table 1). This separation among phenotypically defined populations was also confirmed by a majority of the MEP/Platelet specific genes (Figure 2e, Supplementary Tables 2, 3, 4, 5), and was similar to that observed before transplantation (Supplementary Figure 4d). Thus, undivided PreME/PreMeg cells obtained after transplantation express genes typically restricted to megakaryocyte-erythroid progenitors.

For an in-depth comparative analysis of the transplanted undivided cells (Figure 2) and non-transplanted cells (Supplementary Figure 4), we performed tSNE [42] and hierarchical cluster analysis on gene expression data (Figure 3a-b). We wondered whether HSCs and PreMegs truly form distinctive subgroups in terms of their gene expression profile. Therefore, we excluded the intermediate cell differentiation stages (colored in green) and provided the algorithm with a number of expected clusters (k = 2). Figure 3b illustrates that not only the visual inspection of the t-SNE visualization but also the k-means cluster algorithm is able to distinguish between those two cell types. As expected, while our results reveal a close association between the before- and after- transplantation HSC or PreMeg populations, HSCs and PreMegs themselves form distinct clusters. Therefore, changes in the HSC phenotype before cell division reflect gene expression changes associated with differentiation.

HSCs differentiate into restricted progenitors before entering the S phase of the cell cycle

While the cell tracing dye allowed us to follow cell division, it did not give information on cell cycle progression. Therefore, to determine in which phase of the cell cycle HSCs make fate decisions, we scored each cell for its likely cell cycle phase using signatures for G1, S/G2/M phases [39]. We categorized

144 individual cells in the G0/G1 or the S/G2/M phases (Figure 4a) based on the average expression of phase
145 specific genes [39,43]. As expected, and later confirmed by expression of individual cell cycle genes (Figure
146 4b), HSCs were more quiescent, with almost one-third of the PreME/PreMeg cells still in the G0/G1
147 phases (Figure 4a). We also confirmed cluster separation between cells in G0/G1 and S/G2/M phases by
148 performing t-SNE analysis based on all 15 measured cell cycle genes but restricted to PreME/PreMeg
149 populations (Figure 4c). Next, to determine if the expression of MEP/platelet genes is dependent on
150 progression through the S/G2/M phases, we again used t-SNE analysis to compare PreME/PreMeg cells
151 in the G0/G1 and S/G2/M phases. Remarkably, there was no separation of cells according to their cell
152 cycle status (Figure 4c), suggesting that PreME/PreMeg cells had previously upregulated differentiation
153 genes in the G0/G1 phases of the cell cycle. That PreME and PreMeg cells increase expression of lineage
154 specific genes independent of cell cycle phase, was further supported by comparing the mean expression
155 of MEP/Platelet genes between cells in G0/G1 and S/G2/M phases (Figure 4d). Indeed, PreME and
156 PreMeg cells increase expression of the lineage specific genes independent of cell cycle phases. These
157 data imply that transplanted HSCs differentiate before entering the S phase of the cell cycle.

158 To corroborate these findings, we used the recently described $Ki67^{RFP}$ knock-in mice [44]. KI67 is a nuclear
159 protein that is absent in the G0 phase, starts to be synthesized at the beginning of the S phase, increases
160 until mitosis, and gradually decreases thereafter in the G1 phase of the daughter cells until re-entry into
161 the S phase [45]. We first confirmed that none of the RFP^- cells (LSK or MP) was in the $S/G_2/M$ phase,
162 (Supplementary Figure 6a), and that only RFP^+ cells incorporated BrdU (Supplementary Figure 6b).
163 Using an antibody against KI67, we found that RFP^+ expression truly reflects KI67 expression at the
164 protein level (Supplementary Figure 6c). Thus, $Ki67^{RFP}$ knock-in mice are an appropriate tool to trace cell
165 cycle progression in hematopoietic cells.
166 To follow HSCs through cell cycle progression and differentiation, we sorted RFP^- HSCs residing in the
167 G0/G1 phases, labeled them with CellTrace Violet, and transplanted these cells into non-conditioned
168 recipients. Our results reveal that the majority of donor undivided MPs did not upregulate RFP expression

(Figure 4e), thus remaining in the G0/G1 phases. When taken together with the above results, these findings demonstrate that HSCs do not require S phase entry to become phenotypic MPs.

Functional differences between undivided HSCs and progenitors

We used *in vitro* colony assays to verify functional differences between undivided phenotypic HSCs and MPs due to changes in gene expression profiles. Undivided donor HSCs (LSK $CD48^-$ $CD150^+$) and PreMegs (Lin^- $Sca\text{-}1^-$ Kit^+ $CD150^+$ $CD41^+$) were isolated at 36h after transplantation and cultured as single cells in the presence of growth factors (SCF, TPO, IL-3 and EPO) [46]. Twelve days later, 89% of HSCs were multipotent and gave rise to all cell types (myeloid, erythroid, and megakaryocyte), whereas 92% of the PreMegs differentiated into megakaryocytes alone, clearly suggesting that this population had lost their multipotency (Figure 5a).

We further investigated the *in vivo* repopulating capacity of donor cells. For this, we sorted undivided donor GFP^+ LSK and MP cells obtained at 36h after transplantation, injected them into non-conditioned recipients, and re-transplanted the same amount of cells into lethally irradiated wild type mice (Figure 5b-c). Although both populations gave rise to long-lived erythroid cells, only mice transplanted with LSKs displayed donor-derived GFP^+ short-lived neutrophils and platelets at 3 weeks after transplantation (Figure 5b-d). These observations imply that hematopoietic progenitor cells that down-regulate Sca-1 without prior cell division, as expected, exhibit a dramatic reduction in their repopulation capacity.

Discussion

In this study, we demonstrated *in vivo* that HSCs can differentiate into ST-HSCs, MPPs, and even restricted myeloid progenitors, before undergoing cell division. Using a cell tracing approach and $Ki67^{RFP}$ knock-in mice, we followed HSC differentiation *in vivo* and analysed the expression of several essential megakaryocyte-erythroid and myeloid specific genes, and cell-cycle genes, at the single-cell level. Our findings using undivided PreMegs reveal that phenotypic and gene expression changes in undivided but

differentiated progenitors are accompanied by loss of multipotency and repopulation capacity after transplantation. Based on restricted PreME and PreMeg progenitors as an example of differentiated cells, we reveal that HSCs can initiate a specific differentiation program in the G0/G1 phases, which is before the actual physical division of the cell.

HSCs are rare cells that give rise to numerous blood cell types through a series of intermediate progenitors [4]. Multipotent and restricted progenitors intensively proliferate, making them the key amplifiers of cell numbers in the hematopoietic system [3]. The currently accepted model of hematopoiesis holds that HSCs have to divide in order to produce multipotent and lineage-restricted progenitor populations [3,47,48]. Thus, with respect to HSCs, proliferation and differentiation are currently characterized as simultaneous processes, however, to date, no direct *in vivo* proof of this concept has been provided. On the contrary, it is also conceivable that proliferation and differentiation exist as two independent processes. A few *in vitro* studies have supported this argument and have suggested that HSC division and differentiation are parallel processes. Indeed, while Mossadegh-Keller and colleagues [49] have shown that the myeloid transcription factor PU.1 is induced during the first cell cycle after *in vitro* stimulation of HSCs with M-CSF, Yamamoto and colleagues [6] reported that HSCs can divide asymmetrically and give rise to restricted long-term repopulating megakaryocyte progenitors even after the first division. Kent and colleagues [50] have shown that HSCs down regulated a number of transcription factors responsible for self-renewal division and lost long-term repopulation capacity before first division *in vitro*. Using a single cell sequencing approach, Yang and colleagues demonstrated that HSCs can express megakaryocyte and granulocyte specific genes during the G1 phase of the cell cycle [51]. However, no *in vivo* studies on the possible uncoupling of HSC fate decision and cell cycle progression are currently available.

Indeed, the idea that cells can make fate decisions in the G1 phase of the cell cycle is not new. Pluripotent stem cells (PSCs) initiate differentiation during progression through the G1 phase [14] due to the presence of a ‘window of opportunity’, which is dependent on epigenetic changes that occur during that phase. On the other hand, PSCs maintain their pluripotent state during the S and G2 phases of the cell cycle, which

is regulated by the cell cycle machinery but is independent of the G1 phase [17]. G1 phase specific cell cycle regulators such as cyclin D directly regulate the localization of differentiation transcriptional factors in PSCs [52]. Our results suggest a similar mechanism, which governs cell fate decisions in embryonic pluripotent and multipotent adult stem cells. Moreover, our data are also in line with another report, which demonstrated that division and differentiation of B cells into plasma cells were temporally separated with no significant influence on each other [53].

In summary, we show that HSC division and their differentiation are probably independent processes and that HSCs make fate decisions before entering the S phase of the cell cycle. Additionally, these results open new directions in determining the factors that influence HSCs fate decisions in connection with cell cycle progression during normal hematopoiesis and pathologies associated with abnormal differentiation.

References

1 Oguro, H., Ding, L. & Morrison, S. J. SLAM family markers resolve functionally distinct subpopulations of hematopoietic stem cells and multipotent progenitors. *Cell stem cell* **13**, 102-116, doi:10.1016/j.stem.2013.05.014 (2013).

2 Wilson, A. *et al.* Hematopoietic stem cells reversibly switch from dormancy to self-renewal during homeostasis and repair. *Cell* **135**, 1118-1129, doi:10.1016/j.cell.2008.10.048 (2008).

3 Busch, K. *et al.* Fundamental properties of unperturbed haematopoiesis from stem cells in vivo. *Nature* **518**, 542-546, doi:10.1038/nature14242 (2015).

4 Sawai, C. M. *et al.* Hematopoietic Stem Cells Are the Major Source of Multilineage Hematopoiesis in Adult Animals. *Immunity* **45**, 597-609, doi:10.1016/j.immuni.2016.08.007 (2016).

5 Nestorowa, S. *et al.* A single cell resolution map of mouse haematopoietic stem and progenitor cell differentiation. *Blood*, doi:10.1182/blood-2016-05-716480 (2016).

6 Yamamoto, R. *et al.* Clonal analysis unveils self-renewing lineage-restricted progenitors generated directly from hematopoietic stem cells. *Cell* **154**, 1112-1126, doi:10.1016/j.cell.2013.08.007 (2013).

7 Haas, S. *et al.* Inflammation-Induced Emergency Megakaryopoiesis Driven by Hematopoietic Stem Cell-like Megakaryocyte Progenitors. *Cell Stem Cell*, doi:10.1016/j.stem.2015.07.007 (2015).

8 Hoppe, P. S. *et al.* Early myeloid lineage choice is not initiated by random PU.1 to GATA1 protein ratios. *Nature* **535**, 299-302, doi:10.1038/nature18320 (2016).

9 Paul, F. *et al.* Transcriptional Heterogeneity and Lineage Commitment in Myeloid Progenitors. *Cell* **163**, 1663-1677, doi:10.1016/j.cell.2015.11.013 (2015).

10 Velten, L. *et al.* Human haematopoietic stem cell lineage commitment is a continuous process. *Nat Cell Biol* **19**, 271-281, doi:10.1038/ncb3493 (2017).

11 Cabezas-Wallscheid, N. *et al.* Identification of regulatory networks in HSCs and their immediate progeny via integrated proteome, transcriptome, and DNA Methylome analysis. *Cell Stem Cell* **15**, 507-522, doi:10.1016/j.stem.2014.07.005 (2014).

12 Guo, G. *et al.* Mapping cellular hierarchy by single-cell analysis of the cell surface repertoire. *Cell Stem Cell* **13**, 492-505, doi:10.1016/j.stem.2013.07.017 (2013).

13 Haghverdi, L., Buettner, F. & Theis, F. J. Diffusion maps for high-dimensional single-cell analysis of differentiation data. *Bioinformatics* **31**, 2989-2998, doi:10.1093/bioinformatics/btv325 (2015).

14 Pauklin, S. & Vallier, L. The cell-cycle state of stem cells determines cell fate propensity. *Cell* **155**, 135-147, doi:10.1016/j.cell.2013.08.031 (2013).

15 Singh, A. M. *et al.* Cell-Cycle Control of Bivalent Epigenetic Domains Regulates the Exit from Pluripotency. *Stem cell reports* **5**, 323-336, doi:10.1016/j.stemcr.2015.07.005 (2015).

16 Dalton, S. Linking the Cell Cycle to Cell Fate Decisions. *Trends in cell biology* **25**, 592-600, doi:10.1016/j.tcb.2015.07.007 (2015).

17 Gonzales, K. A. *et al.* Deterministic Restriction on Pluripotent State Dissolution by Cell-Cycle Pathways. *Cell* **162**, 564-579, doi:10.1016/j.cell.2015.07.001 (2015).

18 Lange, C., Huttner, W. B. & Calegari, F. Cdk4/cyclinD1 overexpression in neural stem cells shortens G1, delays neurogenesis, and promotes the generation and expansion of basal progenitors. *Cell stem cell* **5**, 320-331, doi:10.1016/j.stem.2009.05.026 (2009).

19 Laurenti, E. *et al.* CDK6 levels regulate quiescence exit in human hematopoietic stem cells. *Cell stem cell* **16**, 302-313, doi:10.1016/j.stem.2015.01.017 (2015).

20 Mende, N. *et al.* CCND1-CDK4-mediated cell cycle progression provides a competitive advantage for human hematopoietic stem cells in vivo. *J Exp Med* **212**, 1171-1183, doi:10.1084/jem.20150308 (2015).

21 Matsumoto, A. *et al.* p57 is required for quiescence and maintenance of adult hematopoietic stem cells. *Cell stem cell* **9**, 262-271, doi:10.1016/j.stem.2011.06.014 (2011).

22 Zou, P. *et al.* p57(Kip2) and p27(Kip1) cooperate to maintain hematopoietic stem cell quiescence through interactions with Hsc70. *Cell stem cell* **9**, 247-261, doi:10.1016/j.stem.2011.07.003 (2011).

23 Gekas, C. & Graf, T. CD41 expression marks myeloid-biased adult hematopoietic stem cells and increases with age. *Blood* **121**, 4463-4472, doi:10.1182/blood-2012-09-457929 (2013).

24 Miyawaki, K. *et al.* CD41 Marks the Initial Myelo-Erythroid Lineage Specification in Adult Mouse Hematopoiesis: Redefinition of Murine Common Myeloid Progenitor. *Stem Cells* **33**, 976-987, doi:DOI 10.1002/stem.1906 (2015).

25 Roch, A., Trachsel, V. & Lutolf, M. P. Brief Report: Single-Cell Analysis Reveals Cell Division-Independent Emergence of Megakaryocytes From Phenotypic Hematopoietic Stem Cells. *Stem Cells* **33**, 3152-3157, doi:10.1002/stem.2106 (2015).

26 Bernitz, J. M., Kim, H. S., MacArthur, B., Sieburg, H. & Moore, K. Hematopoietic Stem Cells Count and Remember Self-Renewal Divisions. *Cell* **167**, 1296-1309 e1210, doi:10.1016/j.cell.2016.10.022 (2016).

27 Pina, C. *et al.* Inferring rules of lineage commitment in haematopoiesis. *Nat Cell Biol* **14**, 287-294, doi:10.1038/ncb2442 (2012).

28 Quah, B. J. C. & Parish, C. R. New and improved methods for measuring lymphocyte proliferation in vitro and in vivo using CFSE-like fluorescent dyes. *J Immunol Methods* **379**, 1-14, doi:10.1016/j.jim.2012.02.012 (2012).

29 Shimoto, M., Sugiyama, T. & Nagasawa, T. Numerous niches for hematopoietic stem cells remain empty during homeostasis. *Blood* **129**, 2124-2131, doi:10.1182/blood-2016-09-740563 (2017).

30 Cao, X. *et al.* Irradiation induces bone injury by damaging bone marrow microenvironment for stem cells. *Proc Natl Acad Sci U S A* **108**, 1609-1614, doi:10.1073/pnas.1015350108 (2011).

31 Abbuehl, J. P., Tatarova, Z., Held, W. & Huelsken, J. Long-Term Engraftment of Primary Bone Marrow Stromal Cells Repairs Niche Damage and Improves Hematopoietic Stem Cell Transplantation. *Cell stem cell* **21**, 241-255 e246, doi:10.1016/j.stem.2017.07.004 (2017).

32 Schaue, D., Kachikwu, E. L. & McBride, W. H. Cytokines in radiobiological responses: a review. *Radiat Res* **178**, 505-523, doi:10.1667/RR3031.1 (2012).

33 Wilson, N. K. *et al.* Combined Single-Cell Functional and Gene Expression Analysis Resolves Heterogeneity within Stem Cell Populations. *Cell Stem Cell* **16**, 712-724, doi:10.1016/j.stem.2015.04.004 (2015).

34 Pronk, C. J. *et al.* Elucidation of the phenotypic, functional, and molecular topography of a myeloerythroid progenitor cell hierarchy. *Cell Stem Cell* **1**, 428-442, doi:10.1016/j.stem.2007.07.005 (2007).

35 Takizawa, H., Regoes, R. R., Boddupalli, C. S., Bonhoeffer, S. & Manz, M. G. Dynamic variation in cycling of hematopoietic stem cells in steady state and inflammation. *The Journal of experimental medicine* **208**, 273-284 (2010).

36 Pietras, E. M. *et al.* Chronic interleukin-1 exposure drives haematopoietic stem cells towards precocious myeloid differentiation at the expense of self-renewal. *Nat Cell Biol* **18**, 607-618, doi:10.1038/ncb3346 (2016).

37 Schoedel, K. B. *et al.* The bulk of the hematopoietic stem cell population is dispensable for murine steady-state and stress hematopoiesis. *Blood* **128**, 2285-2296, doi:10.1182/blood-2016-03-706010 (2016).

38 Gottgens, B. Regulatory network control of blood stem cells. *Blood* **125**, 2614-2620, doi:10.1182/blood-2014-08-570226 (2015).

39 Kowalczyk, M. S. *et al.* Single-cell RNA-seq reveals changes in cell cycle and differentiation programs upon aging of hematopoietic stem cells. *Genome research* **25**, 1860-1872, doi:10.1101/gr.192237.115 (2015).

40 Klimmeck, D. *et al.* Transcriptome-wide profiling and posttranscriptional analysis of hematopoietic stem/progenitor cell differentiation toward myeloid commitment. *Stem cell reports* **3**, 858-875, doi:10.1016/j.stemcr.2014.08.012 (2014).

41 Moignard, V. *et al.* Characterization of transcriptional networks in blood stem and progenitor cells using high-throughput single-cell gene expression analysis. *Nat Cell Biol* **15**, 363-372, doi:10.1038/ncb2709 (2013).

42 van der Maaten, L. & Hinton, G. Visualizing Data using t-SNE. *Journal of Machine Learning Research* **9**, 2579-2605 (2008).

43 Whitfield, M. L. *et al.* Identification of genes periodically expressed in the human cell cycle and their expression in tumors. *Mol Biol Cell* **13**, 1977-2000, doi:10.1091/mbc.02-02-0030. (2002).

44 Basak, O. *et al.* Mapping early fate determination in Lgr5+ crypt stem cells using a novel Ki67-RFP allele. *The EMBO journal* **33**, 2057-2068, doi:10.15252/embj.201488017 (2014).

45 Scholzen, T. & Gerdes, J. The Ki-67 protein: from the known and the unknown. *Journal of cellular physiology* **182**, 311-322, doi:10.1002/(SICI)1097-4652(200003)182:3<311::AID-JCP1>3.0.CO;2-9 (2000).

46 Grinenko, T. *et al.* Clonal expansion capacity defines two consecutive developmental stages of long-term hematopoietic stem cells. *J Exp Med* **211**, 209-215, doi:10.1084/jem.20131115 (2014).

47 Eaves, C. J. Hematopoietic stem cells: concepts, definitions, and the new reality. *Blood* **125**, 2605-2613, doi:10.1182/blood-2014-12-570200 (2015).

48 Sun, J. *et al.* Clonal dynamics of native haematopoiesis. *Nature* **514**, 322-327, doi:10.1038/nature13824 (2014).

49 Mossadegh-Keller, N. *et al.* M-CSF instructs myeloid lineage fate in single haematopoietic stem cells. *Nature* **497**, 239-243, doi:10.1038/nature12026 (2013).

50 Kent, D. G., Dykstra, B. J., Cheyne, J., Ma, E. & Eaves, C. J. Steel factor coordinately regulates the molecular signature and biologic function of hematopoietic stem cells. *Blood* **112**, 560-567, doi:10.1182/blood-2007-10-117820 (2008).

51 Yang, J. *et al.* Single cell transcriptomics reveals unanticipated features of early hematopoietic precursors. *Nucleic acids research* **45**, 1281-1296, doi:10.1093/nar/gkw1214 (2017).

52 Singh, A. M. *et al.* Signaling network crosstalk in human pluripotent cells: a Smad2/3-regulated switch that controls the balance between self-renewal and differentiation. *Cell stem cell* **10**, 312-326, doi:10.1016/j.stem.2012.01.014 (2012).

53 Duffy, K. R. *et al.* Activation-induced B cell fates are selected by intracellular stochastic competition. *Science* **335**, 338-341, doi:10.1126/science.1213230 (2012).

54 Bonifacio, E. *et al.* Effects of high-dose oral insulin on immune responses in children at high risk for type 1 diabetes: the Pre-POINT randomized clinical trial. *JAMA* **313**, 1541-1549, doi:10.1001/jama.2015.2928 (2015).

55 Fuchs, Y. F. *et al.* CD8+ T cells specific for the islet autoantigen IGRP are restricted in their T cell receptor chain usage. *Sci Rep* **7**, 44661, doi:10.1038/srep44661 (2017).

56 McDavid, A. *et al.* Modeling bi-modality improves characterization of cell cycle on gene expression in single cells. *PLoS Comput Biol* **10**, e1003696, doi:10.1371/journal.pcbi.1003696 (2014).

Acknowledgements

TG received support from the Fritz Thyssen foundation (10.14.2.153). BW was supported by the Heisenberg program (Deutsche Forschungsgemeinschaft – DFG, Germany; WI3291/ 5-1). This work was supported by grants from the DFG (SFB655 “Cells into Tissues” to TC and GR4857/1-1 to TG), a CRTD seed grant to TG and BW and a European Research Council grant (683145) to TC. The work of LT and IG was supported by the German Federal Ministry of Research and Education, Grant number 031A315 “*MessAge*”. We would like to thank Dr. Vasuprada Iyengar for critically reading the manuscript.

Author Contributions

Conceptualization, T.G. and B.W.; investigation, A.K., S.D., and T.G.; methodology, T.G., A.E., L.T., B.R., M.B., A.G. and I.G.; resources, T.G., B.W., O.B. and H.C.; writing original draft, T.G. and B.W.; Writing, review and editing, T.G., B.W., I.G., L.T. T.C. and A.E.; funding acquisition T.G., B.W., L.T., T.C. and I.G.; Supervision, T.G., B.W. and T.C.

We do not have any competing financial interests.

Materials and Methods

Mice. C57BL/6 (B6), B6.SJL-PtprcaPep3b/BoyJ (B6.SJL), HSC-CreERT/R-DTA and Ubc:GFP mice were purchased from the Jackson Laboratory. $Ki67^{RFP}$ knock-in mice have been described before [44]. All mice were bred and maintained under specific pathogen–free conditions in the animal facility at the Medical Theoretical Center of the University of Technology, Dresden. Experiments were performed in accordance with the German animal welfare legislation and were approved by local authorities.

Cre-activation. One week before the start of TAM administration, mice were kept on low phytoestrogen standard diet (LASvendi, Solingen, Germany). 30 mg tamoxifen tablets (Ratiopharm, Ulm, Germany) were dissolved overnight in lipid emulsion (SMOFlipid, Fresenius Kabi, Bad Homburg, Germany). 20 mg/ml tamoxifen solution was applied two times (72h apart) by oral gavage at a dose of 0.2mg / g body weight to animals at the age of 8 – 14 weeks.

Transplantation. Bone marrow was isolated from mouse tibia, femora, pelvis, and vertebrae, crushed, and filtered through a 70-µm cell strainer. Cells were lysed in ACK Lysis Buffer (Life technologies at. A10492-01), and lineage depleted using biotinylated antibodies (anti-mouse CD3 (2C11; 17A2), CD11b (M1/70), CD19 (1D3), CD45R (RA3-6B2), Gr-1 (RB6-8C5), Nk1.1 (PK136)) and anti-biotin micro-beads using magnetic cell separation (Miltenyi Biotec Germany Cat. 130-090-485). Cells were then stained with antibodies and CellTrace Violet dye (Molecular Probes Cat. C34557) according to manufacturer's instructions. Cells were sorted on a FACS Aria II or III (BD Bioscience). 3600 HSCs (Lin^- $Sca\text{-}1^+$ Kit^+ (LSK) $CD48^-$ $CD41^-$ $CD150^+$), 5000 MPP2 (LSK $CD48^+$ $CD150^+$), or 10000 MPP3/4 (Lin^- LSK $CD48^+$ $CD150^-$) cells were transplanted via intravenous injection into non-conditioned C57BL/6 mice. CD4+CD62L+ naïve T cells (10^6), labeled with CellTrace Violet, were transplanted as controls for 'undivided cells. Lymph node donor cells were analyzed 36h after transplantation along with LSK cells. For transplantation of cells from $Ki67^{RFP}$ knock-in mice, RFP^- cells were sorted and donor BM cells were analyzed 36h after transplantation, based on CellTrace Violet staining. For competitive transplantation, 20 GFP^+ LSK cells or MPs (Lin^- $Sca\text{-}1^-$ Kit^+) were sorted 36h after a primary

transplantation of 3600 HSCs from Ubc-GFP mice into unconditioned recipient C57BL/6 mice. LSKs and MPs were transplanted together with 10^5 non-fractionated BM cells from B6.SJL mice into lethally irradiated (900 cGy) C57BL/6 wild-type recipients.

Flow cytometry. All analyses were done on FACS Aria II and Canto (BD Bioscience). The antibodies used for staining are CD117 (2B8), Sca-1 (D7), Ter119 (Ter119), CD41 (MWReg30), CD48 (HM48-1), CD105 (MJ7/18), CD16/32 (93), CD11b (M1/70), Gr-1 (RB6-8C5), all from eBioscience, CD150 (TC15-12F1; BioLegend).

Single-cell index sorting. Isolated cells were single-cell sorted into 8-well strips containing 5µl of PBS. To record marker levels of each cell, the FACS Diva-7 "index sorting" function was activated during cell sorting. Using index sorting, single cells were sorted from the entire Lin^- Kit^+ CellTrace $Violet^+$ space, and the intensities of the Cell Trace Violet, Kit, Sca-1, CD41, CD48, CD150, CD105, and CD16/32 FACS markers recorded and linked to each cell's position.

Cytospins. Cells were spun onto object slides at 500 RPM, dried and stained with May-Grunwald and Gimza solution (Sigma Aldrich).

In vitro culture. Single cells were sorted and cultured in 96 well plates in StemSpan SFEM medium (STEMCELL Technologies, Cat. 09600) supplemented with 20 ng/ml rmSCF (Peprotech, 250-03), 20 ng/ml rmTpo (eBioscince, 34-8686-63), 20 ng/ml rmIl3 (Peprotech, 213-13), and 5 U/ml rhEpo (Roche), and cultivated for 12 days at 37^0C with 5% CO_2.

Cell cycle analyses. For intracellular staining, cells were fixed and permeabilized using fixation and permeabilization buffers from eBioscience. To distinguish between the G0 and G1 phase, cells were stained for intracellular Ki-67 FITC (eBiosciences, clone SolA15). DAPI (4, 6 diamidino-2-phenylindole; Molecular Probes) was used to measure DNA content and separate the cells in S/G2/M phases from those in the G0 and G1 phase. For the BrdU incorporation assay, 10µM BrdU (Sigma-Aldrich) was added to the culture for 3.5 h and BrdU incorporation analyses performed as described previously [46] using anti-BrdU-FITC ab (eBioscience, clone BU20a).

Clustering based analysis of cell cycle state. Cell cycle genes were classified based on single cell deep sequencing data [39] or defined previously in synchronized HeLa cells [43] (G1 phase genes: Ccne1, Cdk2, Cdkn1a, Cdkn1c, S/G2/M phase genes: Cdkn2d, E2f4, Cdk6, Cdkn2c, Ccng2, Ccnf, Mki67, Ccna2, Ccnb1, Ccnb2, Cdc20). First, expression of each gene for each cell was normalized to the maximum expression of the gene; second, cell cycle signature for each cell was defined as the average expression of phase specific subsets of cell cycle genes. Discrimination between G1 and S/G2/M was done based on the distribution of control HSCs (before transplantation) and data that around 90% of HSCs (mouse strain C57Bl6) are in G0/G1 phase of the cell cycle.

Single-cell qPCR. Gene expression profiles of single cells were obtained as previously described [54,55] but with modifications. cDNA was synthesized directly on the cells using the Quanta qScript TM cDNA Supermix. Total cDNA was pre-amplified for 20 cycles (1x 95ºC 5', 95ºC 45'', 60ºC, 1', 72ºC 1.5') and once at 68ºC for 10' using the Multiplex PCR Kit (Qiagen, Hilden, Germany) in a final volume of 35 µl in the presence of primer pairs (25nM for each primer) for all genes (listed in Table S1). Pre-amplified cDNA (10 µl) was then treated with 1.2 U Exonuclease I and gene expression quantified by real time PCR on the BioMark™ HD System (© Fluidigm Corporation, CA, USA) using the 96.96 Dynamic Array IFC, the GE 96x96 Fast PCR+ Melt protocol, the SsoFast EvaGreen Supermix with Low ROX (BIO RAD, CA, USA), and 5 µM primers, for each assay. Raw data were analyzed using the Fluidigm Real-Time PCR analysis software.

Bioinformatics analysis. Pre-processing and data analysis of single-cell expression profiles were conducted using KNIME 2.11.2, R Version 3.3.2 and RStudio Version 0.99.486 and version 1.0.136 (Boston, MA, USA) software. Where further required, pre-processing via a linear model to correct for confounding sampling effects was conducted as previously described [54]. t-SNE plots were created using the R package 'Rtsne'. To model the bi-modal gene expression of single cells, the Hurdle model, a semi-continuous modeling framework, was applied to pre-processed data [56]. This allowed us to assess differential expression profiles as a function of frequency of expression and mean positive expression

using a likelihood ratio test. k-means clustering for k=2 was performed on the normalized data and using the R package 'stats'.

Statistical analysis. Data were expressed as mean +/- standard deviation (s.d.). Statistical analyses based on unpaired Student's t test were performed using Prism 5.0 software (GraphPad). P value <0.05 were considered as statistical significant.

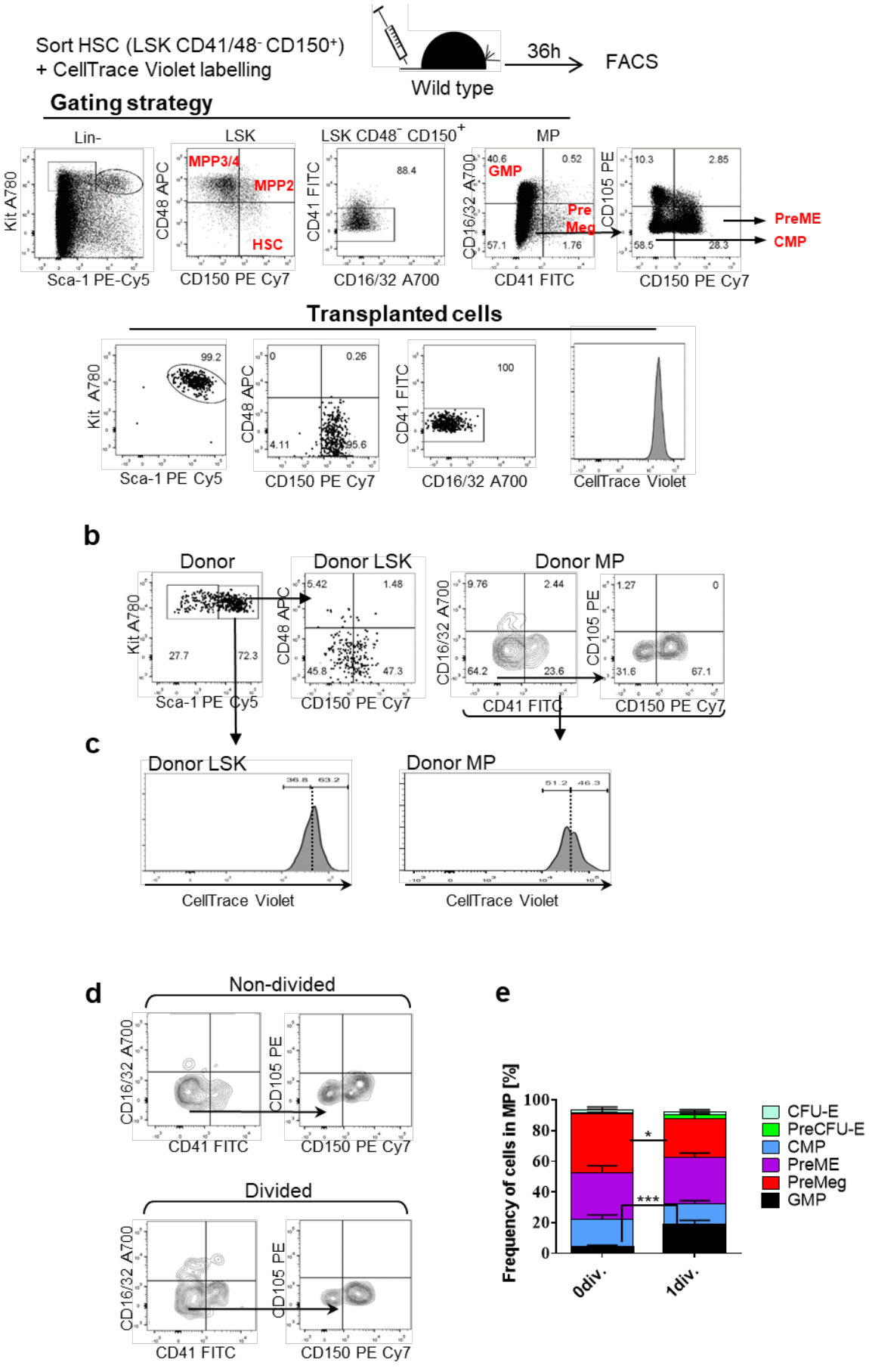

491

Figure 1. Differentiation and division proliferation history of HSCs after transplantation into non-conditioned recipients.

(a) HSCs (LSK CD48$^-$ CD41$^-$ CD150$^+$) were labelled with CellTrace Violet dye and 3600 cells were transplanted into non-conditioned wild type mice. Purity of transplanted cells was more than 99% for each experiment. **(b)** Bone marrow was harvested at 36h after transplantation and recipient cells were analyzed using indicated gates. **(c)** Dilution of CellTrace Violet in donor LSK and MPs, 36h after transplantation. Labelled and transplanted naïve CD62L$^+$CD4$^+$ T cells were used as reference for undivided cells. 500 donor cells were analyzed from 11 transplanted mice, representative data for one out of 13 experiments **(d)** Phenotype of undivided and divided donor MPs (n=11), representative example of 13 independent experiments. **(e)** Frequency of restricted progenitors in undivided ('0' div.) and divided (1 div.) donor MPs, pooled data from 13 independent experiments. Unpaired Student t-test, data are means +/- S.D., P***=0.0002, P*=0.02.

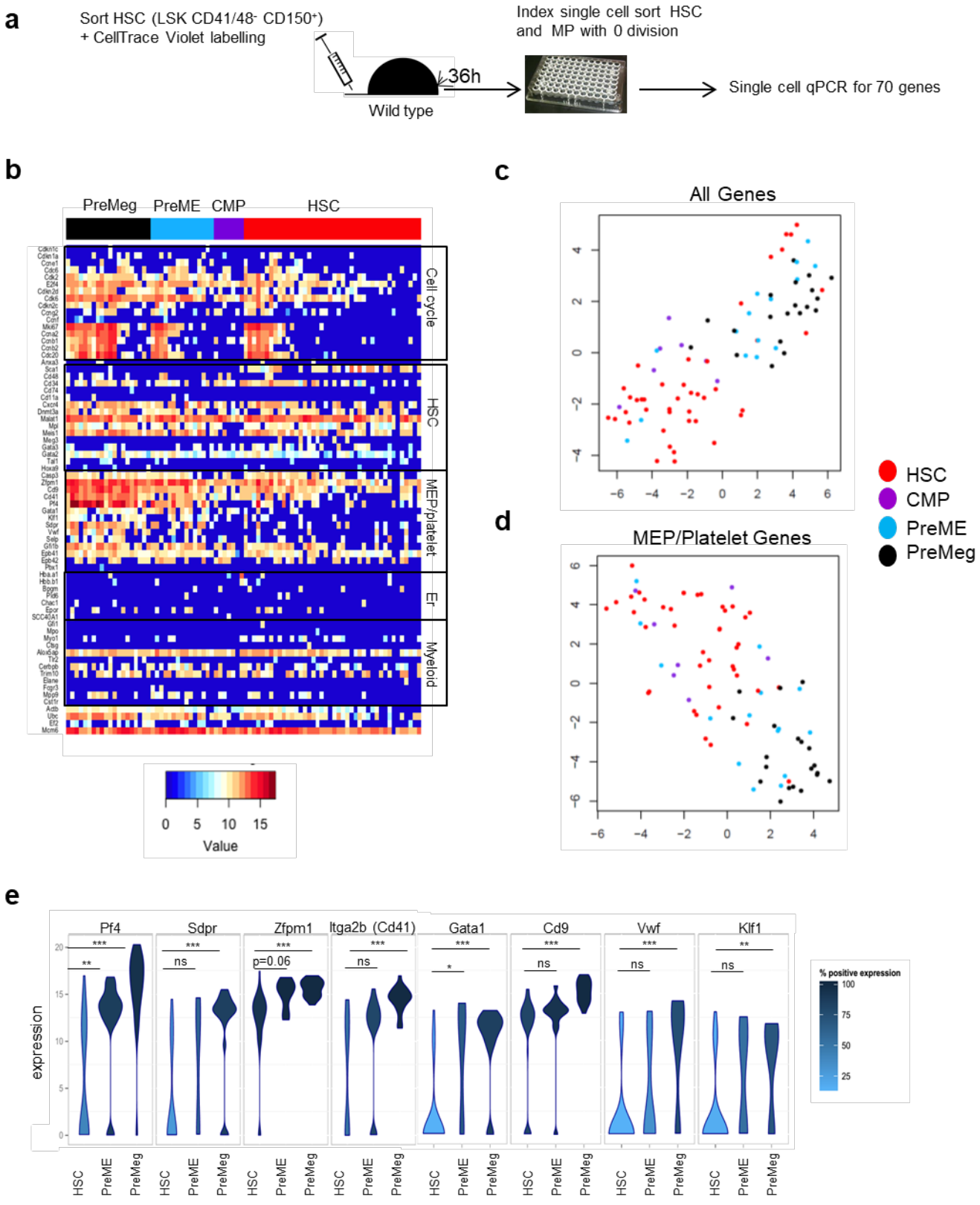

Figure 2. Single cell expression analysis in undivided donor HSCs and MPs.

(a) Experimental design. LSK $CD48^-$ $CD41^-$ $CD150^+$ cells were transplanted into non-irradiated recipients, and single, undivided donor Lin^- Kit^+ cells were sorted using the index sort approach at 36h after transplantation. Data from two independent experiments (n= 12 mice). Based on index sort data, HSCs were defined as LSK $CD48^-$ $CD150^+$; CMPs as Lin^- Kit^+ $Sca\text{-}1^-$ $CD16/32^-$ $CD41^-$ $CD150^-$ $CD105^-$; PreME as Lin^- Kit^+ $Sca\text{-}1^-$ $CD16/32^-$ $CD41^-$ $CD150^+$ $CD105^-$; and PreMeg as Lin^- Kit^+ $Sca\text{-}1^-$ $CD16/32^-$ $CD41^+$ $CD150^+$ $CD105^-$. All sorted 42 HSC, 7 CMP, 15 PreME and 20 PreMeg cells were analyzed. **(b)** Heat map showing gene expression analysis. Each row corresponds to a specific gene, each column corresponds to a specific and individual donor cell, and colors represent expression levels of individual genes (dCt). **(c)** t-SNE plot for all analyzed genes and cells, axes have arbitrary units. **(d)** t-SNE plot for MEP/Platelet genes for all cells, axes have arbitrary units. **(e)** Violin density plots for the most differently expressed MEP/Platelet genes. Y-axis represents gene expression. The horizontal width of the plot shows the density of the data along the Y-axis. Statistical significance was determined using the Hurdle model. *($p<0.05$), **($p<0.01$), ***($p<0.0001$), ns (not significant). Data from 2 independent experiments, n=12. Exact P value in supplemental Tables S2-3.

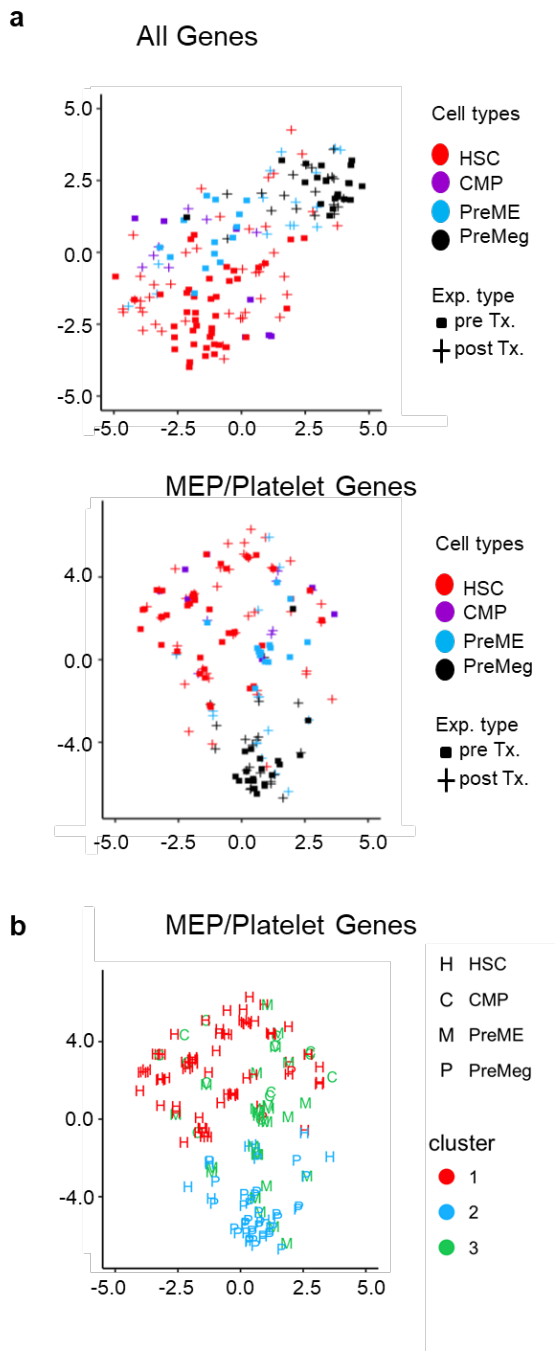

Figure 3. Comparison of gene expression between cells before transplantation and undivided cells after transplantation.

(a) t-SNE plot for all analyzed genes (top panel) and MEP/Platelet genes (bottom panel) for all cells before transplantation and undivided donor cells at 36h after transplantation. Axes display arbitrary units.

525 **(b)** t-SNE visualization for all cells before transplantation and all undivided cells after transplantation
526 (36h). The color coding depicts the results of a reproducible k-means clustering (k=2) on all cells before
527 and after transplantation based on MEP/Platelet genes.

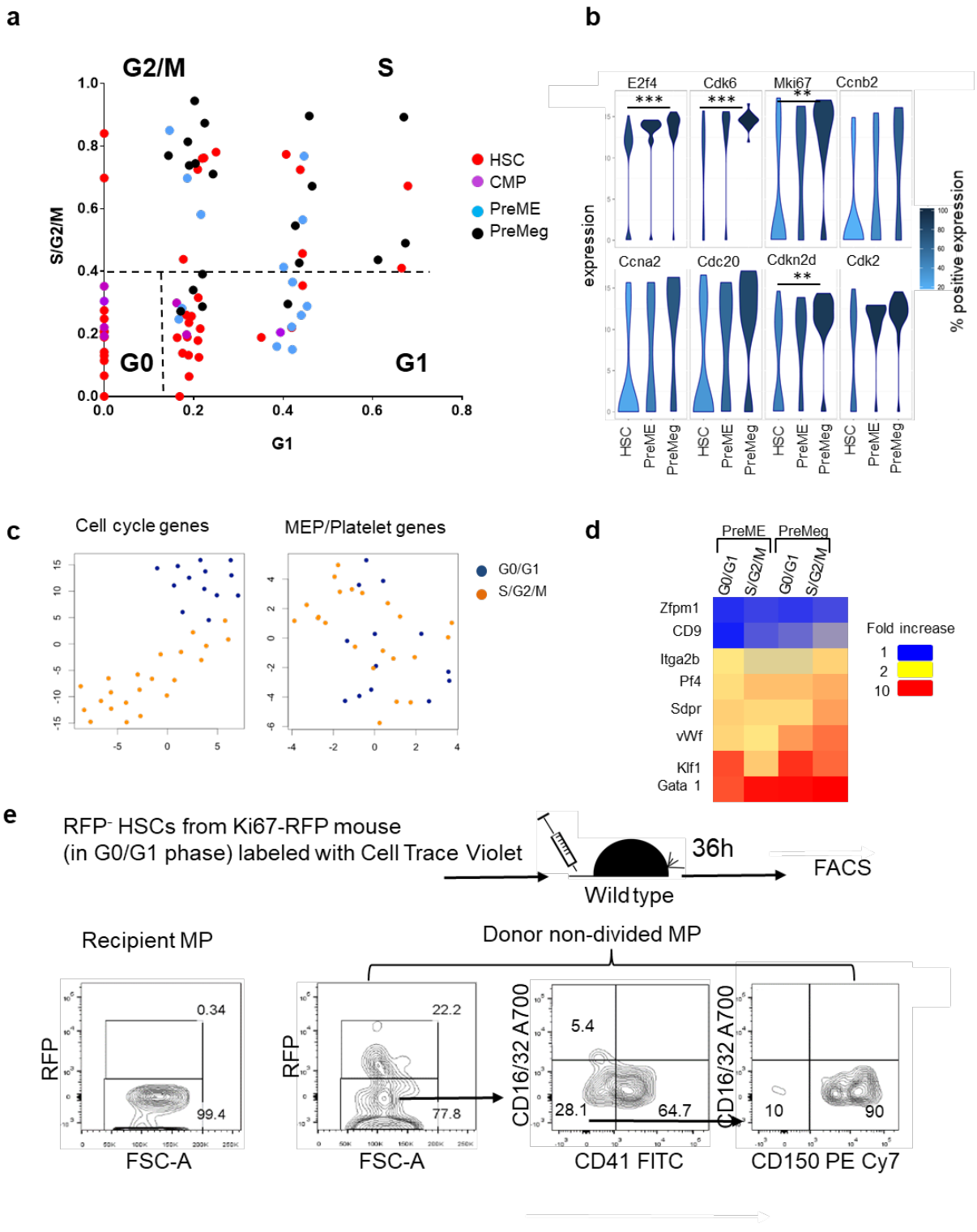

528

529 **Figure 4. Cell cycle distribution of undivided donor HSCs, CMPs, PreMEs, and PreMegs.**

(a) Prediction of cell cycle phases for all undivided donor cells 36h after transplantation. Shown is the average expression of G1 genes (x-axis) and S/G2/M genes (y-axes) **(b)** Violin density plots for the most differently expressed cell cycle genes. Y-axis represents gene expression. The horizontal width of the plot shows the density of the data along the Y-axis. Statistical significance was determined using the Hurdle model. *($p<0.05$), **($p<0.01$), ***($p<0.0001$). Exact P value in supplemental Tables 2-3. **(c)** t-SNE plots for PreME/ PreMeg cells based on cell cycle genes and MEP/Platelet genes. **(d)** Mean expression of MEP/Platelet genes was calculated for HSCs, PreMEs and PreMegs in G0/G1 and S/G2/M phases and is depicted as fold-increase relative to mean expression in HSCs in the G0/G1 phases. **(e)** RFP expression in undivided donor MPs at 36h after transplantation of RFP^- HSCs from $Ki67^{RFP}$ knock-in mice. Recipient MPs were used as negative controls for RFP expression. (Representative example, n=5, from 2 independent experiments).

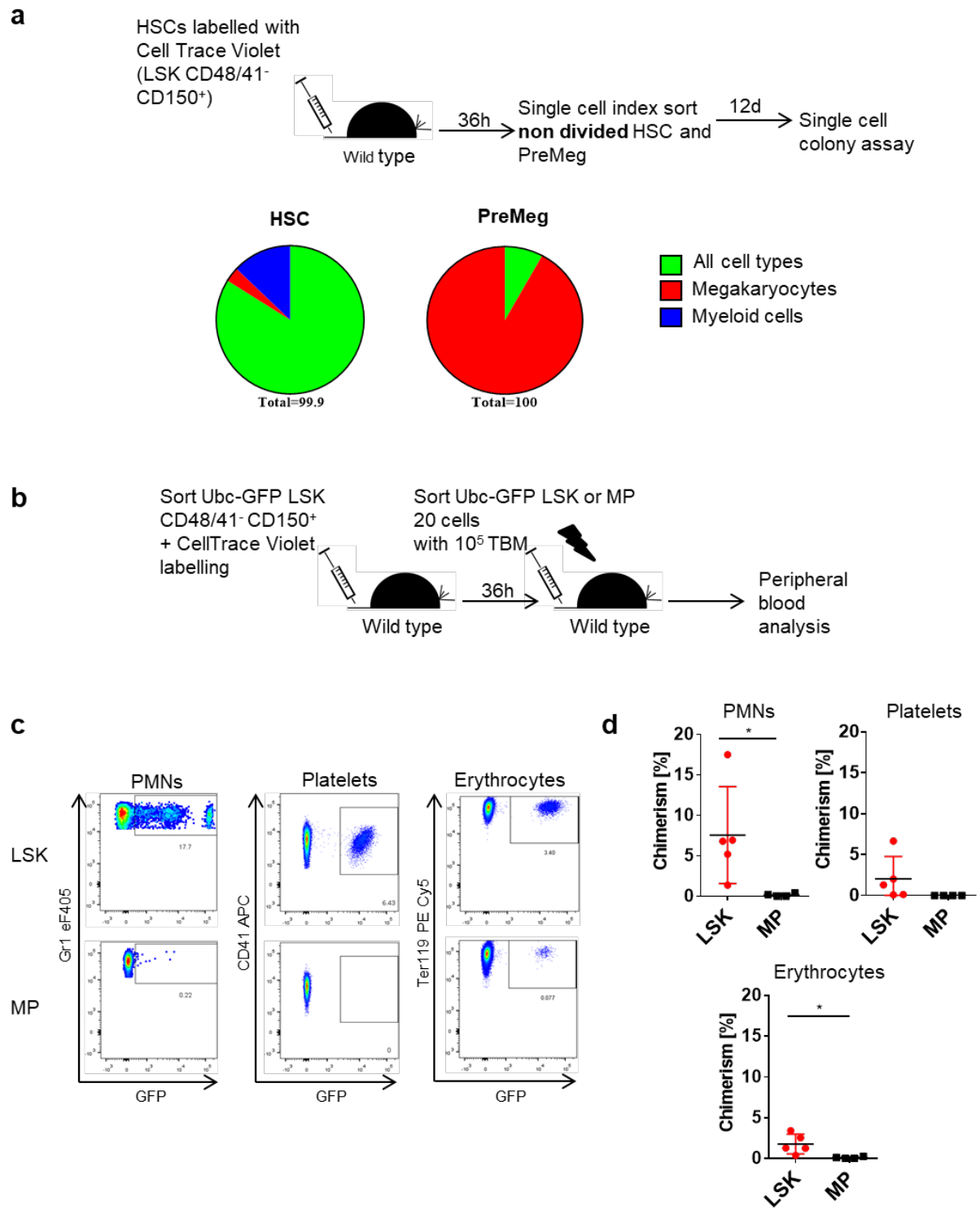

541

542 **Figure 5. Functional analysis of undivided donor HSCs and MPs.**

543 **(a)** Individual undivided donor HSCs (LSK $CD48^-$ $CD150^+$) and PreMeg (Lin^- $Sca\text{-}1^-$ Kit^+ $CD41^+$
544 $CD150^+$ $CD16/32^-$) cells were sorted 36h after transplantation and cultivated in liquid culture media
545 supplemented with mSCF, mTPO, mIl3 and hEpo. Cell composition was analyzed after 12 days using
546 May-Grunwald-Giemsa staining. Colonies (n=31) for HSCs and (n=25) PreMegs, 3 independent
547 experiments, 15 mice. 82% HSCs generated colonies (more than 20 cells) and 79% PreMegs generated
548 more than 3 megakaryocytes. **(b)** Reconstitution experiment using Ubc-GFP mice. **(c)** Peripheral blood
549 analysis at 3 weeks after secondary transplantation into lethally irradiated recipients. Donor cell
550 contribution to peripheral blood neutrophils (PMNs) $CD11b^+$ $Gr1^+$, platelets $Ter119^-$ $CD41^+$, and
551 erythrocytes $Ter119^+$. Representative plots and pictures from 2 independent experiments (n=5). We
552 checked the mice every 3-4 weeks for a period of 16 weeks after transplantation, but did not find any
553 repopulation from MPs. **(d)** Quantification of peripheral blood analysis from 2 independent experiments,
554 n=5. Statistical significance was determined using unpaired Student's t-test *($p<0.05$). Data are means +/-
555 S.D.
556